American Mineralogist, Volume 62, pages 1003–1005, 1977

Paraspurrite, a new polymorph of spurrite from Inyo County, California

ALAN A. COLVILLE

Department of Geology, California State University,
Los Angeles, California 90032

AND PATRICIA A. COLVILLE

Cyprus Research Company, Los Angeles, California 90064

Abstract

Paraspurrite, $Ca_5(SiO_4)_2CO_3$, a new polymorph of spurrite, is monoclinic with a = 10.473(10), b = 6.706(5), c = 27.78(3)A., β= 90.58(7)°, space group $P2_1/a$ and Z = 8. Paraspurrite occurs in a small lens in a sequence of thermally-metamorphosed calc-silicates near Darwin, California. Associated minerals include gehlenite, vesuvianite, apatite, and larnite.

Introduction

A routine powder pattern run for identification of a mineral from a calc-silicate body near Darwin, California, showed first-order agreement with the X-ray powder pattern reported for spurrite (Powder Data File 13/496), but with some additional reflections. Single-crystal oscillation and precession photographs showed that these crystals are indeed closely related crystallographically to spurrite, but differ principally by having a doubled unit cell in the c^* direction.

The new mineral was found by Mr. Norm Nichols in a sequence of thermally-metamorphosed siliceous carbonate rocks in Inyo County, California, north of the small mining town of Darwin. Paraspurrite occurs as a distinctive part of a small roof pendant. Direct contact with syenite can be observed along most of the margin of the pendant, but the contact is obscured on one side by cinders from overlying volcanics.

Spurrite itself is not a common mineral, but it is important as a critical phase in the spurrite–melilite facies of contact metamorphism. This facies is characterized by formation at low pressures and at temperature conditions which are high for near-surface environments, that is, 800° to perhaps as high as 1000°C. The mineral assemblage typically is undersaturated in silica and includes such phases as spurrite, tilleyite, merwinite, rankinite, and larnite. The rocks are usually marbles with carbonate sedimentary rocks as their parents.

Mineralogy

Paraspurrite occurs as the dominant phase of a dark-gray granulite-facies rock which exhibits conspicuous fracturing. The intergrown paraspurrite crystals average about 0.5 cm across and reach a maximum size of about 2.0 cm. The crystals are colorless in thin section and many exhibit polysynthetic twinning on (001). Cleavage is poor parallel to (001). Paraspurrite is biaxial (−) with α = 1.650, β = 1.672, γ = 1.677, $2V_\alpha$ = 47°; $X = b$, $Z \wedge C$ = 30°. $Y \wedge a$ = 30°.

Microanalyses were carried out on the Materials Analysis Company model 5-SA3 electron microprobe. The program ULTIMATE was used for control of the microprobe and for data reduction (Chodos *et al.*, 1973). The chemical analysis (Table 1) confirms that the formula, $Ca_5 (SiO_4)_2CO_3$, is identical to that of spurrite.

Examination of representative thin sections was augmented by X-ray powder data to determine the associated minerals. Gehlenite, vesuvianite, and apatite are relatively abundant; and larnite is less common. An apparent second generation of minerals includes calcite, quartz, gypsum, and pyrite. In contact with the lenticular body of paraspurrite is a zone of massive grossular.

X-ray crystallography

Precession photographs provided crystal geometry, systematic extinctions, and preliminary cell parameters. A single crystal of paraspurrite was mounted

Table 1. Paraspurrite. Chemical data

Chemical Analysis		Electron Microprobe Analysis	
SiO_2	27.25	SiO_2	26.73
Al_2O_3	0.37	Al_2O_3	.00*
Fe_2O_3	0.12	FeO	.01*
TiO_2	0.02	TiO_2	.00*
CaO	62.78	CaO	62.13
MgO	0.19	MgO	.03*
Na_2O	0.03	Na_2O	.04*
K_2O	---	BaO	.04*
P_2O_5	0.13		
MnO	0.02	TOTAL	88.86
Loss on Ignition	8.65 [T.G.A. 8.97]		
TOTAL	99.88		

*Below limit of detectability

parallel to *a**. Upper-level photographs confirmed that paraspurrite is monoclinic with *a* = 10.52, *b* = 6.76, *c* = 27.7A and β= 90.58°. On the basis of the systematic absences, the space group is $P\ 2_1/a$.

Accurate cell parameters were calculated using a least-squares analysis of 15 reflections measured with an automated four-circle single-crystal diffractometer. The final cell parameters and other crystal data are compared to those of spurrite in Table 2.

Table 2. Spurrite and paraspurrite. Comparison of crystal data

	Spurrite	Paraspurrite
a	10.49Å	10.473(10)Å*
b	6.705Å	6.706(5)Å
c	14.15Å	27.78(3)Å
β	101.32°	90.58(7)°
V	975.9Å^3	1951.(2)Å^3
Z	4	8
Space group	$P2_1/a$	$P2_1/a$
Sp. Gr. (exp)	3.025	3.00
Sp. Gr. (calc)	3.01	3.01
Strong x-ray lines**	2.701 (100), 2.635 (70), 3.019 (65), 2.663 (50), 2.170 (40), 3.81 (30)	3.47 (100), 6.95 (78), 1.983 (63), 2.698 (48), 2.647 (39)

*Cell parameters are from data collected with single crystal diffractometer

**d-spacing (Å) and relative intensity

Table 3. Powder data for paraspurrite

hkl*	d(calc)	d(obs)**	I/Io	hkl	d(calc)	d(obs)	I/Io
004	6.95	6.92	78	404	2.442	2.443	8
012	6.04	6.03	34	00.12	2.315	2.313	28
$20\bar{1}$	5.15	5.15	14	$22\bar{7}$	2.307	2.307	12
201	5.13	5.12	27	227	2.295	2.292	
006	4.63	4.62	37	$40\bar{6}$	2.288	2.288	4
203	4.54	4.54	2	$20.\overline{11}$	2.284	2.282	2
$21\bar{1}$	4.087	4.09	2	406	2.268	2.268	4
211	4.078	4.08	2	20.11	2.265	2.262	6
$20\bar{5}$	3.829	3.83	11	$03\bar{2}$	2.208	2.208	6
016	3.81	3.82	12	01.12	2.188	2.186	8
205	3.78	3.80	12	$41\bar{6}$	2.165	2.165	7
$21\bar{3}$	3.78	3.78	8	416	2.149	2.149	8
213	3.758	3.76	5	02.10	2.139	2.140	2
008	3.47	3.47	100	408	2.080	2.080	17
020	3.355	3.35	16	420	2.064	2.065	5
215	3.301	3.30	4	$231;23\bar{1}$	2.050	2.050	4
$20\bar{7}$	3.18	3.18	12	036	2.014	2.015	8
018	3.08	3.08	4	$23\bar{3}$	2.009	2.008	5
024	3.02	3.017	20	$00.14;42\bar{4}$	1.983	1.983	63
026	2.717	2.716	42	02.12	1.905	1.905	4
$22\bar{3}$	2.706	2.707	34	$42\bar{6}$	1.891	1.890	10
223	2.698	2.698	48	$22.\overline{11}$	1.888	1.887	5
$20\bar{9}$	2.671	2.671	25	$03\bar{8}$	1.880	1.880	7
209	2.647	2.647	39	426	1.879	1.879	7
400	2.617	2.617	8	428	1.768	1.767	11

* *Use of single-crystal data facilitated indexing of reflections*

** *Brackets enclose peaks with severe overlap. These were measured at the top and* $K\alpha_1$, *was used for d(obs)*

Powder patterns were obtained using a Norelco diffractomer, a copper anode *X*-ray tube, a graphite monochromator, and NaF as an internal standard. Overlapping peaks dominate the pattern because the beta angle is close to 90° and $2\theta_{hkl}$ and $2\theta_{hk\bar{l}}$ are close together for many reflections. Overlap is promoted also by a relatively large unit cell and a primitive lattice. The indexed powder pattern is given in Table 3. The 00*l* reflections show some effect from preferred orientation. The enhancement is not extreme as these are among the strongest reflections on the single-crystal photographs. Reflections with severe overlap are grouped with brackets. The cell parameters listed in Table 2 were used to compute *d*-spacing.

Discussion

Paraspurrite is chemically identical to spurrite and is closely related crystallographically. Note that in paraspurrite *a* and *b* remain essentially the same but *c* = 27.78A and β = 90.58°. In effect, paraspurrite exhibits a *c* axis equal to 2 × d_{001} of spurrite.

The crystal structure of paraspurrite is probably quite similar to that of spurrite; that is, isolated silicon tetrahedra coordinated by Ca atoms as in Ca_2SiO_4, and CO_3^{2-} equilateral triangles also coordinated by Ca atoms as in aragonite (Smith *et al.*, 1960; Kletsova and Belov, 1961). In spurrite there are two independent silicon-oxygen tetrahedra, Si_I and Si_{II}, and five independent calcium-oxygen polyhedra, Ca_I through Ca_V. The space group of paraspurrite

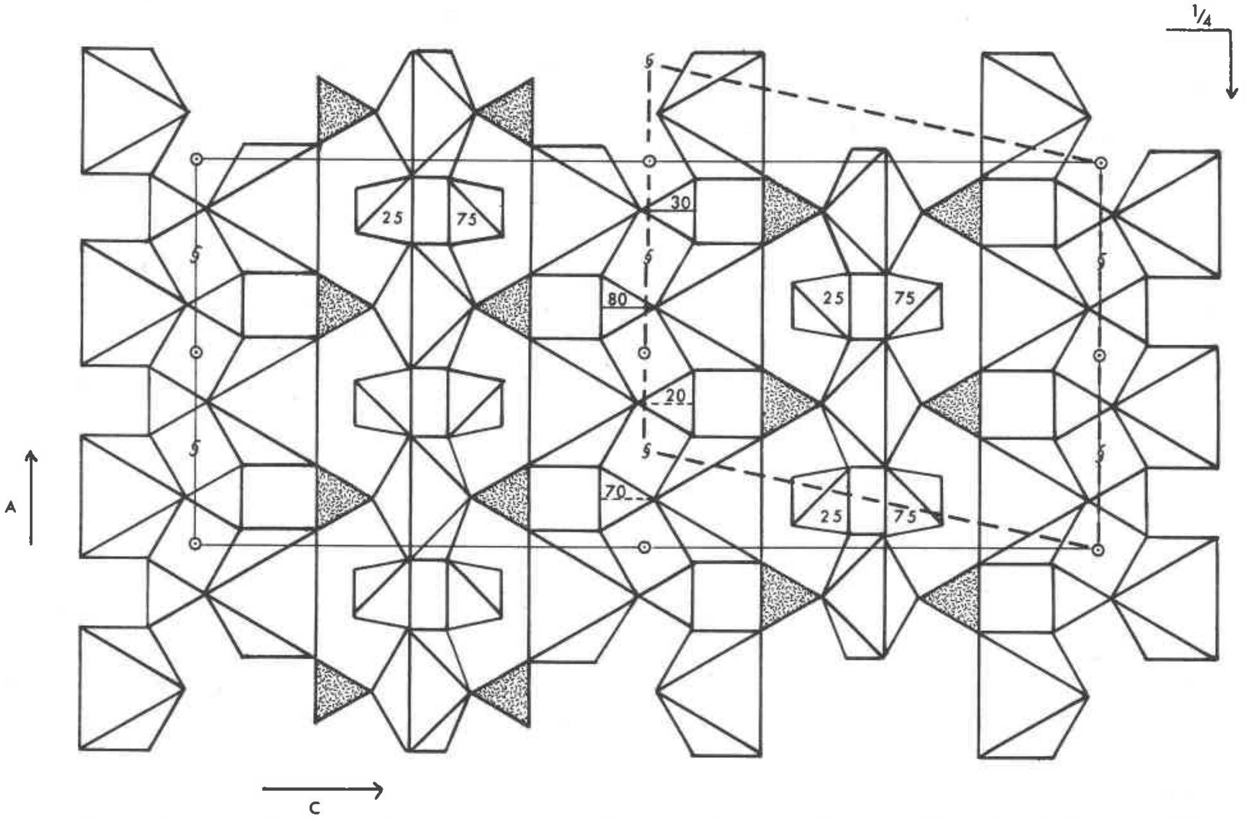

Fig. 1. Proposed structure for paraspurrite projected onto (010) based on diagram of Kletsova and Belov (1961). The monoclinic unit cell of spurrite is outlined by dashed lines for comparison.

($P2_1/a$) dictates that centers of symmetry and screw axes will no longer duplicate adjacent polyhedra such as $\mathrm{Si_I}$ tetrahedra along *a* ($Z = 0$) will not be equivalent to rows of $\mathrm{Si_I}$ tetrahedra at $Z = ½$ in paraspurrite (Fig. 1).

The determination of the topology and coordination geometry of this new structure would provide an interesting comparison to that of spurrite. In particular the comparison of the $\mathrm{Si_{IA}}$ and $\mathrm{Si_{IB}}$, $\mathrm{Si_{IIA}}$, and $\mathrm{Si_{IIB}}$ and the five pairs of Ca-coordination polyhedra would be profitable, but will have to await an accurate crystal structure analysis. Because all 38 atoms are probably in general positions, this would involve an arduous refinement of 114 atomic coordinates, 38 isotropic temperature factors, and the scale factor, for a total of 153 variables. An anisotropic refinement might be impractical because 343 variables would have to be refined.

Name

The Commission of New Minerals and Mineral Names (IMA) approved the name prior to publication. This new mineral is named paraspurrite to indicate its close crystallographic and chemical relationship to spurrite.

Acknowledgments

It is a pleasure to acknowledge Norm Nichols for recognizing in the field that this might be an unusual occurrence and species and to thank him for donating specimens to us for study. We appreciate the help of Robert Stull in optical and petrographic determinations.

References

Chodos, A. A., A. L. Albee, A. J. Gancarz and J. Laird (1973) Optimization of computer controlled quantitative analysis of minerals. *Proc. 8th Conf. Electron Probe Analysis,* New Orleans, 45A–45C.

Klevtsova, R. F. and N. V. Belov (1961) Crystal structure of spurrite. *Soviet Phys.-Crystallogr., 5,* 659–667. [trans. *Kristallografiya, 5,* 689–697 (1960)].

Smith, J. V., I. L. Karle, H. Hauptman and J. Karle (1960) The crystal structure of spurrite, $Ca_5(SiO_4)_2CO_3$. II. Description of structure. *Acta Crystallogr., 13,* 454–458.

Manuscript received, January 6, 1977; accepted for publication, May 13, 1977.